British Geological Survey
NATURAL ENVIRONMENT RESEARCH COUNCIL

IAGA 2005 Scientific Assembly, Toulouse, France.
Session GAV02, Poster C219

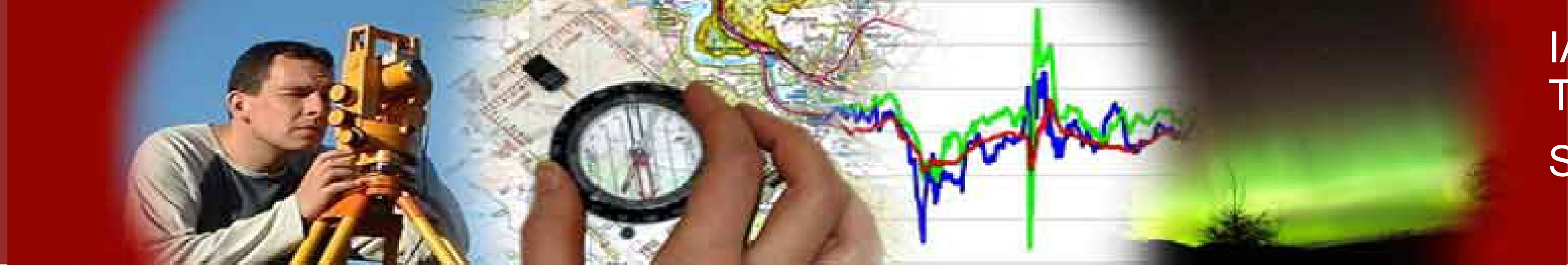

Automated real time detection of solar wind shocks and consequences for the identification of *SSC* and *SI* events

E. Clarke, O. Baillie, A. J. McKay, S. J. Reay, and A. W. P. Thomson

ABSTRACT Algorithms have been developed to automatically detect Earth bound shocks in the solar wind as measured by the ACE satellite. These involve simple threshold techniques and wavelet analysis. One practical application of this shock detection is that it can provide power companies with advanced warning of the potential for geomagnetically induced currents. The automatically detected shocks have been tested against published lists of known shocks and accuracy statistics are presented. Another use for automated shock detection is an aid to the preparation of lists of rapid variations: SSC and SI events. To contribute to the IAGA published list of rapid variations, as prepared by Ebro Observatory, BGS staff routinely identify, scale and classify the events recorded at the three UK magnetic observatories. This is carried out using the criteria from the Atlas of Rapid Variations (1959) and subsequent IAGA instructions. The usefulness of automated detection of solar wind shocks for this task is examined by testing these against lists of identified SSC and SI events.

INTRODUCTION

Shocks in the solar wind can be useful precursors to the onset of magnetic storms. The measurements made on board the NASA ACE spacecraft, located at the L1 point, enables the detection of a shock in the solar wind 20-60 minutes before it's interaction with the Earth's magnetic field. When detected at ground level by magnetometers located at magnetic observatories these are classified either as a Storm Sudden Commencement (*SSC*) or a Sudden Impulse (*SI*). A shock implies an abrupt change in the solar wind characteristics. The most important data for detection are the bulk speed (km/s), the density (particles/cc) and the magnetic field strength (nT) [1]. An example is shown in Figure 1. Certain shock characteristics such as the sign of each of the steps in the data types, can help classify the shocks as fast/slow, forward/reverse shocks. We have developed two shock detection algorithms, which attempt to detect and classify shocks using ACE real time data.

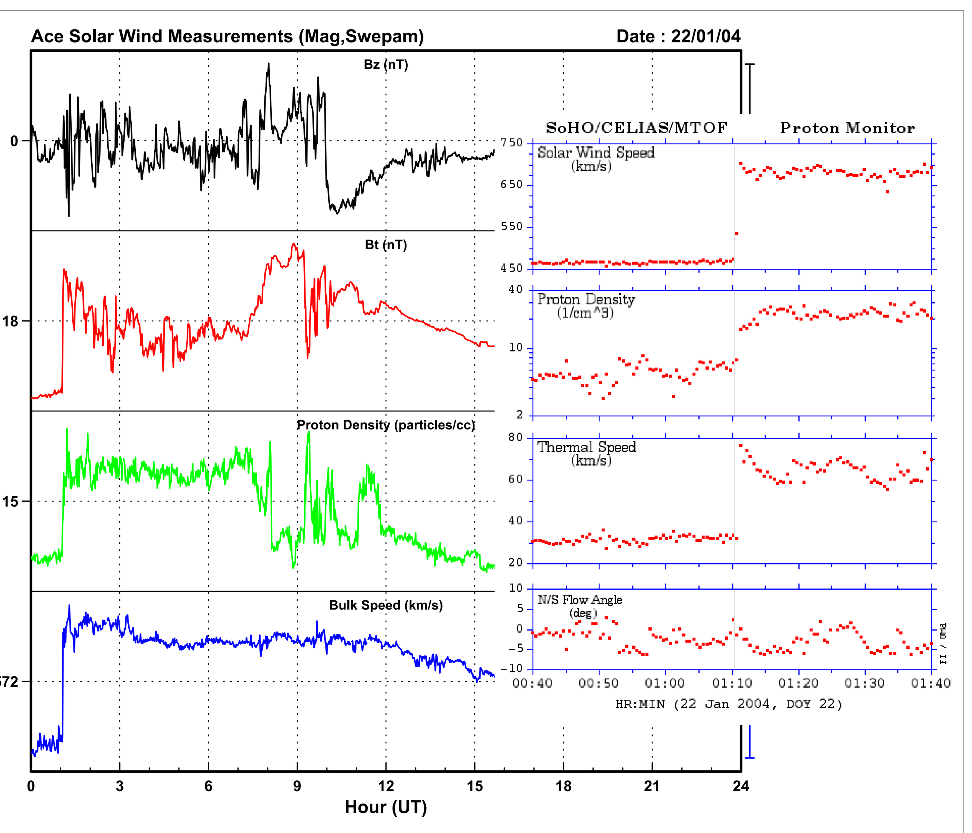

Figure 1: A shock in the solar wind identified in the ACE data by all detection methods and classified as "Fast Forward". Also shown (inset) is the same shock measured by the SOHO spacecraft and classed as "high quality zone 4" by "Shockspotter" [4].

DETECTION BY WAVELET ANALYSIS

Figure 1 suggests a simple step function would be a useful first approximation model. We are trying to detect an edge in the signal and characterise it. A multi-scale edge detector based on the wavelet transform is used [2]. The analysing wavelet is the first derivative of a Gaussian function [3]. For near real time (10 min delay) operation, the first three scales of the transform are used in order to minimise the end effects in the data segment. Shocks, of a given type, are declared if the cross-scale product in each of the appropriate variables exceeds pre-set thresholds. Preliminary thresholds were chosen by reference to a sub-set from two published shock lists [4,5].

DETECTION BY THRESHOLD METHODS

This shock detector works by computing the change in each of the solar wind parameters and dividing by their most recent standard deviations. If this ratio is bigger than pre-defined thresholds a shock is declared. Two separate shock monitors are in operation: the High Q method, which tests for significant changes in solar wind velocity, density, magnetic field strength and the component of velocity normal to the shock front [1]; and the Low Q method, which simply uses the magnetic field strength. The Low Q method is useful during high energy events when the ACE SWEPAM instrument is unable to measure the speed and density of the solar wind.

In Figure 2 we show what is known as the Receiver Operating Characteristic (ROC) for the Low Q method. The ROC shows these data as a function of threshold. The axes of the ROC are the probability of shock detection (POD) and the probability of a false detection (POFD). Threshold levels decrease from left to right and we use this graph to determine the optimum threshold for the method. A high POFD would be unacceptable to most users. We have chosen a compromise that produces low errors but captures most events. The optimum POD and POFD were also established for both the High Q threshold and Wavelet methods in a similar way to that of the Low Q.

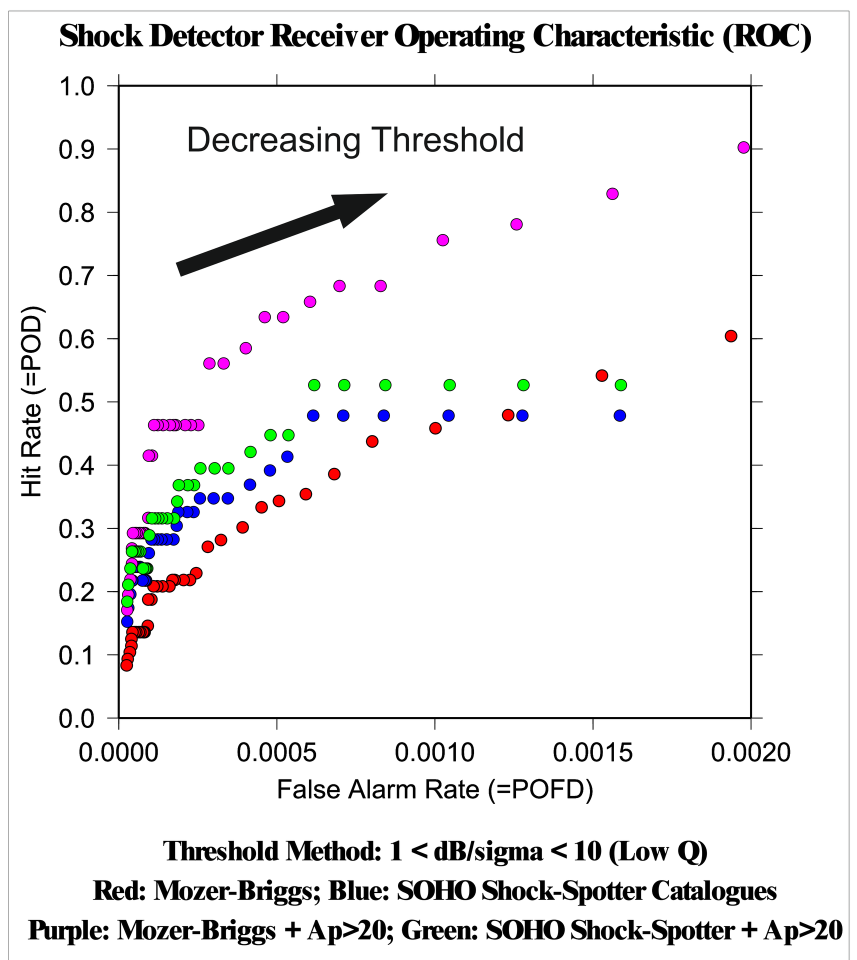

Figure 2. The ROC for the Low Q method. The effectiveness is compared against 4 data sets from 2001 [4,5]. The results in blue [5] are used for determining the threshold levels to use. The optimum performance of the detector occurs at the point furthest from a diagonal line where POD=POFD.

REAL TIME APPLICATION

In 2003 a new system was developed, which built on our work in monitoring and modeling Geomagnetically Induced Current (GIC) for power companies. For the purposes of a warning of likely GIC, the shock detection algorithms discussed here were implemented for real time application. When detected, shocks are posted on the SWIMIC [6] web pages (Figure 3). During office hours BGS staff remove any clear false alarms. This proves necessary as the near real time ACE data are prone to gaps and spikes. The four buttons along the bottom of the page are links to the various GIC services. When a significant event occurs, the relevant button is animated and changes colour as is the case in this example for the solar wind event button (pink).

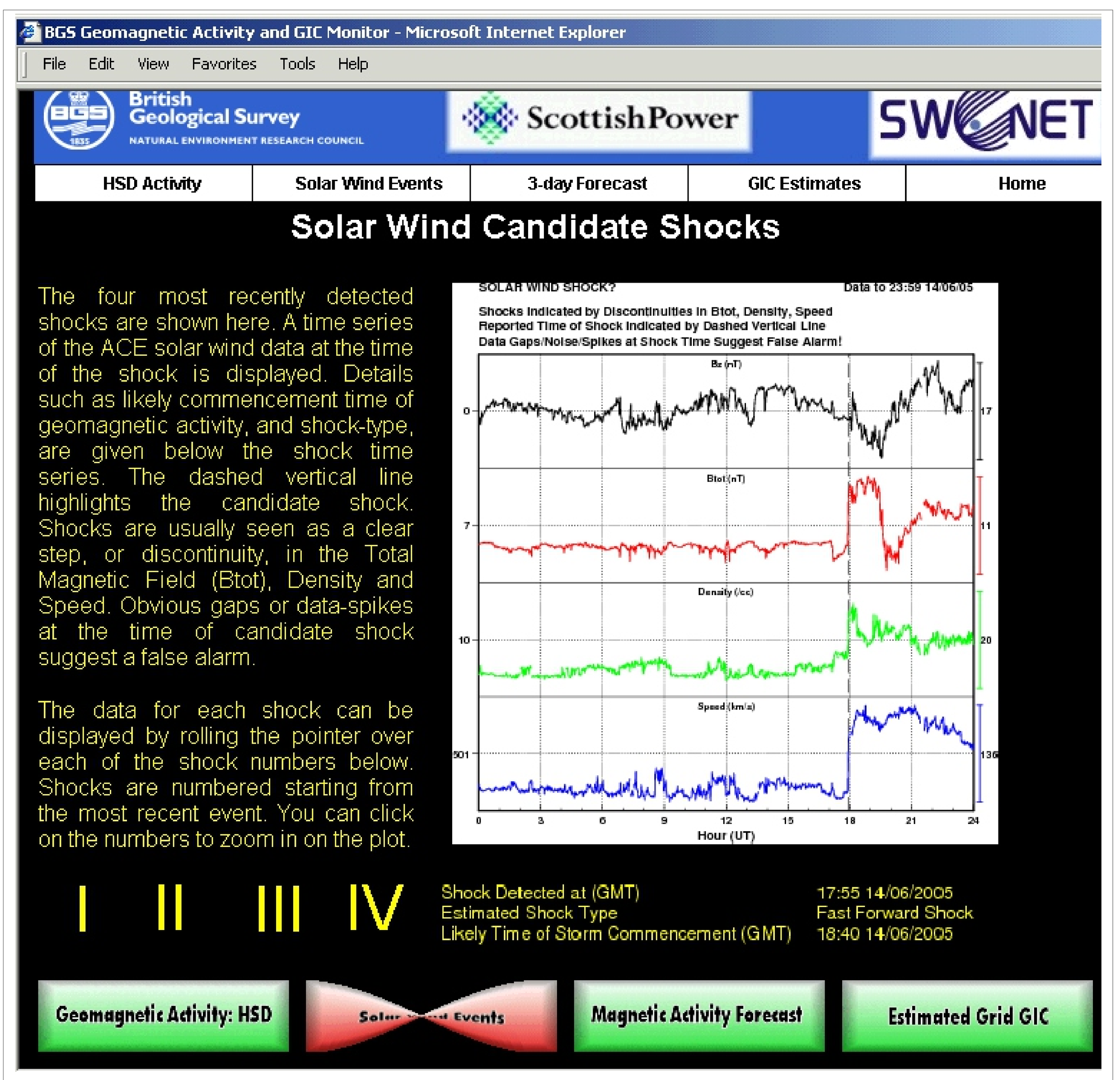

Figure 3. The solar wind shock web page [6]. The dashed line on the plot indicates the estimated time of the shock. At any given time the last four detected shocks can be displayed with the expected SSC time listed at the bottom of the page. The SSC associated with this shock is shown in Figure 4.

SHOCK DETECTION ACCURACY

In order to test the accuracy of the detection methods an independent reference list of shocks has been compiled. We have used the shock events list from [4]. These were originally subjectively identified by eye, using measurements from the SOHO spacecraft, and checked for consistency with the magnetic field behaviour from ACE or WIND spacecrafts. We have then modified this original list by removing those that were not clear shocks and including any extra that were clear shocks as identified by eye in the ACE data. Although we consider this the best available for comparison, it is not a definitive list of shocks and the accuracy results shown here should be considered relative rather than absolute.

Using ACE level 2 data the output for each method has been compared with the reference list over a 5 year period (2000 to 2004) and the results are shown in Table 1. Although the operational detection algorithms use real time ACE data, instead of lower quality, we have used level 2 data in this analysis to determine the results from real physical characteristics rather than those triggered by spikes, which is a separate problem. The results show that both the High Q and the Wavelet methods detect a large majority of the significant shocks. Although the High Q method has the highest percentage of those detected correct, it actually detects fewer numbers in the check list. Combined with Low Q the algorithm detects many more but also has more false alarms. The results for the Wavelet method are probably better balanced.

Table 1 : Accuracy of the shock detection methods as compared to a prepared check list of shocks

Shock Detection Method	Number of shocks detected	Detected Shocks in Check List ?		Check List Shocks Missed ?	
		YES	NO	NO	YES
Check List	176				
High Q	89	85%	15%	43%	57%
High Q and Low Q	181	62%	38%	64%	36%
Wavelets	147	80%	20%	66%	34%
High Q and Wavelets	165	76%	24%	72%	28%

RAPID VARIATIONS

For many years, *SSCs*, like the example shown in Figure 4, and *SIs* recorded at magnetic observatories, have been identified, classified and scaled by observers around the world according to the definitions given in [7] and supplemented in [8]. These events correspond to the solar wind shock arrival at the magnetosphere and are recorded almost simultaneously around the world. Automated methods of shock detection being developed within the community should help to detect, classify and scale these events. If an accurate method can be found it would significantly reduce the time taken for this task and remove the subjectivity that exists in the manual method. In an initial study we have compared the lists of solar wind shocks (2000 to 2004) identified by either the High Q or the Wavelet methods with lists of rapid variations. Both the ISGI collated list of *SSC* and the list of those identified from at least one of the UK observatories are compared. The results are shown in Table 2. The high percentage of correct *SSC* predictions from the check list provides independent evidence to justify it's use as a reference. The poorer results for the automated detection methods suggest they are currently of limited use for *SSC* prediction. Our algorithms also predict the time of the *SSC or SI*.

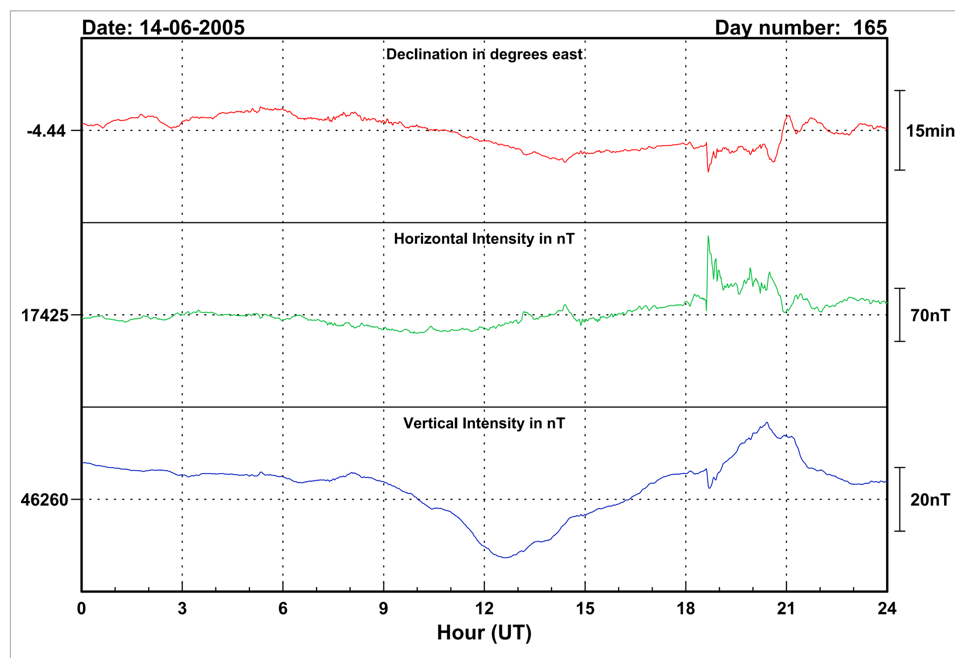

Figure 4: Magnetogram from Eskdalemuir Observatory on 14th June 2005 showing the clear SSC timed at 18:35 UT resulting from the shock detected in Figure 3.

Table 2 : The percentage of shocks that are followed by SSCs. Two lists of SSCs are used in the comparison: i. the ISGI collated list; and ii. the list of SSCs or SIs that have been identified as A or B class [7,8] from at least one of the three UK observatories.

Shock List	Shock followed by ISGI SSC		ISGI SSCs predicted	
Check List	YES = 71%	NO = 29%	YES = 78%	NO = 22%
High Q & Wavelets	YES = 57%	NO = 43%	YES = 58%	NO = 42%
	Shock followed by UK SSC/SI		**UK SSCs/SIs predicted**	
High Q & Wavelets	YES = 48%	NO = 52%	YES = 54%	NO = 46%

We have analysed the accuracy of these predictions over the 5 year period and found that both methods predict an arrival time on average 9 minutes later than the true time. This suggests a simple offset, which will be included in the next software revision.

The results of an investigation into magnetic activity levels following the shocks detected are shown in Figure 5. Only the times when daily *Ap* exceeded the given thresholds on the day of the shock or the day following the shock are counted. We see that the BGS detected shocks are more likely to be followed by magnetic activity. This gives an indication that the current threshold levels, optimised for a power company user, with many of the less clear shocks being missed, also optimises the detection mechanism as a warning of ensuing geomagnetic activity.

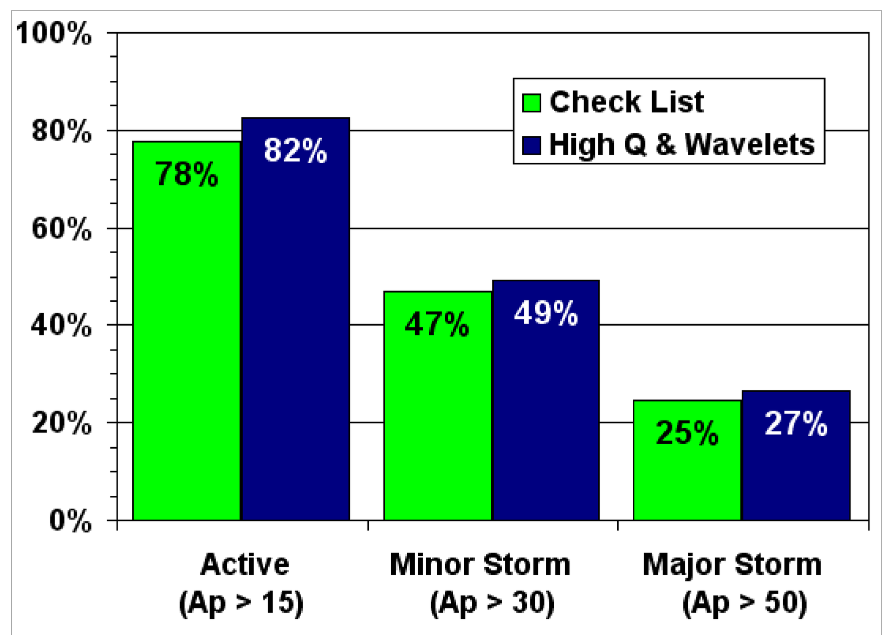

Figure 5 : The percentage of shocks detected by either the High Q or the Wavelet method and those in the check list, that are followed by geomagnetic activity. Three activity levels are shown.

CONCLUSIONS AND FUTURE WORK

We conclude that the current shock detection system is fit for purpose, in that it acts as a warning of likely GIC.

The results of this study suggest some changes to the simple threshold algorithm may be desirable. The High Q method would be improved by lowering some of the thresholds and the Low Q improved by increasing the threshold to lower the number of false alarms. Further analysis of the ROC for both the threshold and the Wavelet detection is recommended, however it should be remembered that the optimum combination of POD and POFD is user specific.

It ought to be possible to automate the identification and scaling of *SSCs* and *SIs*. The results of this study indicate this, although it will not be a simple task, especially if homogeneity of the global *SSC* catalogue is to be maintained. It is more likely that any automatic detection algorithm will still need to be supplemented by a manual decision making process. If the IAGA requirement to measure these events continues, then we plan to develop this work further.

REFERENCES

[1] Burgess, D., *1995. Collisionless Shocks, in Introduction to Space Physics. Kivelson, M. G. and Russell, C.T. (Eds), Cam.Univ.Press.*

[2] Sadler, B.M., Pham, T. and Sadler, L.C., *1998. Optimal and wavelet-based shock wave detection and estimation. J. Acoust. Soc. Am., 104(2): 955-963*

[3] Mallat, S. and Zhong, S., *1992. Characterisation of signals from multiscale edges. IEEE Trans. Pattern. Anal. Mach. Intell., 14: 710-732.*

[4] University of Maryland, *An incomplete list of possible Interplanetary Shocks observed by the PM (SOHO). UMTOF web page http://umtof.umd.edu/pm/Figs.html*

[5] Mozer, J.B., and Briggs, W.M., *2003. Skill in real-time solar wind shock forecasts. J. Geophys. Res.: Space Physics, 108 (A6), SSH 9 p1-9*

[6] Thomson A.W.P., McKay, A.J., Clarke, E. and Reay, S.J., *2005, Surface electric fields and GIC in the Scottish power grid during the 30 October 2003 geomagnetic storm, AGU Space Weather, accepted July 2005. www.geomag.bgs.ac.uk/gicpublic*

[7] Atlas of Rapid Variations. 1959. Ann. IGY, p 694-709.

[8] Mayaud, P.N. *Criteria for the identification of SSCs and definition of the code numbers. 1973., Appendix E of IAGA Bulletin No. 33.*

ACKNOWLEDGMENTS

We would like to thank the following:

- *the ACE SWEPAM instrument team, the ACE MAG instrument team and the ACE Science Center for providing the ACE level 2 data.*
- *NOAA and SEC for the real time provision of ACE solar wind data.*
- *the CELIAS/MTOF experiment on the Solar Heliospheric Observatory (SOHO) spacecraft.*
- *ISGI and Ebre Observatory for the collation and provision of rapid variation data.*
- *ESA for support to carry out the SWIMIC project.*